

Calculation of the Molecular Ordering Parameters of (\pm)-3-Butyn-2-ol Dissolved in an Organic Solution of Poly(γ -benzyl-L-glutamate)

Philippe Lesot, Denis Merlet, and Jacques Courtieu*

Laboratoire de Chimie Structurale Organique, ICMO, URA CNRS no 1384, Université de Paris-Sud, 91405 Orsay, France

James W. Emsley

Department of Chemistry, University of Southampton, Highfield, Southampton SO17 1BJ, United Kingdom

Tapio T. Rantala and Jukka Jokisaari

Department of Physical Sciences Linnanmaa, University of Oulu, 90570 Oulu, Finland

Received: March 12, 1997; In Final Form: May 28, 1997[⊗]

The proton and natural abundance carbon-13 NMR spectra of (\pm)-3-butyn-2-ol enriched in the *S* enantiomer (ee = 72%) and oriented in the *chiral* nematic liquid crystalline phase of [poly(γ -benzyl-L-glutamate)/deuteriochloroform] have been obtained and analyzed. The residual $^1\text{H}-^1\text{H}$ and $^1\text{H}-^{13}\text{C}$ dipolar couplings were corrected for the effects of molecular harmonic vibrational motions and used to determine the r_α structure and the five independent order parameters, $S_{\alpha\beta}$, for each enantiomer. It is shown that the data is consistent with the two enantiomers having an identical r_α structure, but the order matrices differ in both the magnitudes of their elements and the orientation of their principal axes.

Introduction

A new and useful method for enantiomeric analysis, which uses NMR measurements on anisotropic organic solutions of poly(γ -benzyl-L-glutamate) (PBLG), has been described recently.^{1–4} It has been shown that deuterium, proton, fluorine-19, or natural abundance carbon-13 NMR spectra can be used in this way to measure the enantiomeric purity for a wide range of chiral materials bearing various functional groups or chiral molecules with an asymmetric heteroatom.

There are a number of reasons why the NMR spectra of enantiomers in PBLG, or in other liquid crystalline solvents whose constituent molecules are also chiral, should differ, but their relative importance is not yet clear. The differences must arise from intermolecular interactions, with the most obvious effect being the differences in the molecular orientational ordering of the *R* and *S* isomers, i.e. $S_{\alpha\beta}^R \neq S_{\alpha\beta}^S$ (where $\alpha, \beta = a, b, c$). In PBLG solutions, however, the enantiomers are in fast exchange between being surrounded by the organic solvent, when their ordering is negligibly small, to being close to the PBLG polymer, when their ordering is large. A simple, approximate description is that the observed order parameters, $S_{\alpha\beta}^k$, where k is *R* or *S*, are weighted averages of those for bound ($S_{\alpha\beta}^k$)^b, and free molecules, ($S_{\alpha\beta}^k$)^f, and so

$$S_{\alpha\beta}^k = p^k \cdot (S_{\alpha\beta}^k)^b + (1 - p^k) \cdot (S_{\alpha\beta}^k)^f \quad (1)$$

where p^k is the fraction bound.

Assuming that ($S_{\alpha\beta}^k$)^f = 0, then if ($S_{\alpha\beta}^R$)^b = ($S_{\alpha\beta}^S$)^b, the observed order parameters will be different if p^k is different for the two enantiomers, but their magnitudes will be linearly scaled and their principal axis systems (PAS) will be related by a mirror plane. In this case, the chiral discrimination process arises only from a molecular dynamic difference between *R* and *S*. Conversely, if $p^R = p^S$ and ($S_{\alpha\beta}^R$)^b \neq ($S_{\alpha\beta}^S$)^b, then the observed

order parameters, $S_{\alpha\beta}^k$, will be different but not linearly scaled in magnitudes, and their PAS will not be related by a mirror plane.

In addition, the bound molecules may also have an altered geometry from those that are free, and this effect could differ for the two enantiomers. The molecular geometry of the interacting nuclei in each enantiomer affects the magnitudes of the observed dipolar couplings, D_{ij}^k ⁵

$$D_{ij}^k = -\frac{\mu_0 \hbar \gamma_i \gamma_j}{8\pi^2 r_{ij}^3} [S_{cc}^k (3 \cos^2(\varphi_{ij}^c)^k - 1) + (S_{aa}^k - S_{bb}^k) (\cos^2(\varphi_{ij}^a)^k - \cos^2(\varphi_{ij}^b)^k) + 4S_{ab}^k (\cos(\varphi_{ij}^a)^k \cdot \cos(\varphi_{ij}^b)^k) + 4S_{ac}^k (\cos(\varphi_{ij}^a)^k \cdot \cos(\varphi_{ij}^c)^k) + 4S_{bc}^k (\cos(\varphi_{ij}^b)^k \cdot \cos(\varphi_{ij}^c)^k)] \quad (2)$$

where i and j specify the interacting nuclear pair ($i, j = ^1\text{H}, ^{13}\text{C}$), γ_i is the gyromagnetic ratio for the i th nucleus, and (φ_{ij}^a)^k and (φ_{ij}^b)^k define the angles for each enantiomer between the internuclear vectors r_{ij} and a molecular reference axis system (a, b, c)^k.

In order to determine the order parameters and the geometrical factors from the observed dipolar couplings, it is necessary to assume the magnitude of one internuclear distance and to obtain more D_{ij}^k for each enantiomer than there are unknowns in eq 2. There is a further complication in interpreting dipolar couplings in that they are averages over vibrational and bond rotational motion. It is necessary to allow for this averaging in order to decide whether the structures of the bound enantiomers are different from one another.

To establish the importance of the factors giving rise to the differences in the dipolar couplings for pair of enantiomers is a difficult task. It is desirable to obtain a set of D_{ij}^k for each enantiomer that is sufficiently large so that the structure and orientational order parameters can both be obtained. But to do this requires being able to resolve and analyze the complex

[⊗] Abstract published in *Advance ACS Abstracts*, July 1, 1997.

spectra given by a mixture of two compounds. This has not yet been achieved, but a recent study by proton and carbon-13 NMR of the two enantiomers of (\pm)- β -(trichloromethyl)- β -propiolactone (denoted as (\pm)-TMPL) dissolved in a PBLG solution obtained sets of D_{ij}^k which enabled the $S_{\alpha\beta}^k$ to be determined by assuming a fixed geometry for each enantiomer.⁶ Vibrational averaging was not taken into account, but for a rigid molecule this is likely to have a small effect on the derivation of the order parameters $S_{\alpha\beta}^R$ and $S_{\alpha\beta}^S$ and should not alter the main conclusion of this work that the PAS of (\pm)-TMPL are not mirror images, thus demonstrating that the two enantiomers are differently oriented in average in the phase.⁶

In this paper, we describe a proton and natural abundance carbon-13 NMR study of a mixture of the two enantiomers of (\pm)-3-butyn-2-ol (hereafter denoted as (\pm)-BTL) dissolved in the liquid crystalline phase of [PBLG/ $CDCl_3$]. This particular molecule was investigated because there are a large enough set of interacting nuclei that it should be possible to obtain a sufficient number of D_{ij}^k in order to investigate for the first time both structure and orientational order. As we shall see, this has been only partially successful, because of the complexity of the spectra, but it has proved possible to give a more rigorous examination of the factors producing the differences in the NMR spectra of the two enantiomers.

Experimental Section

Sample Preparation. The (\pm) 3-butyn-2-ol was prepared in enantiomeric excess, according to the synthetic scheme described by Michelet et al.⁷ The NMR sample was made from 80 mg of PBLG (DP = 360, MW = 75 000 g \cdot mol⁻¹), 55 mg of a mixture of *S*-enriched (\pm)-BTL (ee = 72%), and 435 mg of $CDCl_3$, which were weighed directly into a 5 mm diameter tube. It should be noted that working with an enantiomeric excess allows the NMR spectra from each enantiomer to be easily identified.⁸ The sample was subjected to four freeze-pump-thaw cycles, before being sealed to avoid the evaporation of deuteriochloroform. It was then centrifuged back and forth until an optically homogeneous birefringent phase was obtained.

NMR Spectroscopy. NMR experiments were performed on a Bruker high resolution spectrometer equipped with a 5 mm diameter $^1H/^{13}C$ dual probe and operating at frequencies of 400.13 MHz for proton and 100.62 MHz for carbon-13. The temperature was maintained at 300 K by the Bruker BVT 1000 system. The deuteriochloroform signal provided the deuterium lock signal. Before the NMR spectra were measured, the sample was kept for about half an hour in the magnetic field in order to achieve a good thermal equilibration. The proton and carbon spectra were recorded using a 90° pulse and collecting 32 and 1500 transients with 16K data points, respectively. For the carbon spectrum, proton irradiation was applied during the relaxation delay period (3 s) to benefit from the nuclear Overhauser effect.

NMR Results

The NMR spectra were analysed with the aid of the simulation program 'PANIC' from Bruker Spectrospin. The numbering of the nuclei in (\pm)-BTL used in this work is shown in Figure 1.

Proton Spectral Analysis. The anisotropic 1H spectrum displayed in Figure 2 is that of a typical A_3MX spin system, which is characterized by the nine spectral parameters ν_i , J_{ij} , and D_{ij} . The magnitudes of the J_{ij} were kept fixed in the iterative analyses at the values obtained from an isotropic solution in $CDCl_3$ at 300 K, and their signs were taken from the literature.⁹ The relative signs of the D_{HH} were determined by performing

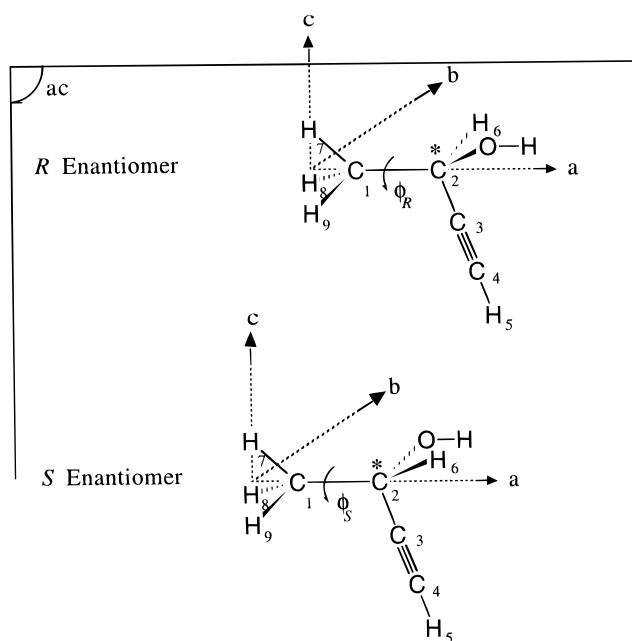


Figure 1. Definition of axes labels (a, b, c)^k of the reference molecular coordinate frame and numbering system of atoms.

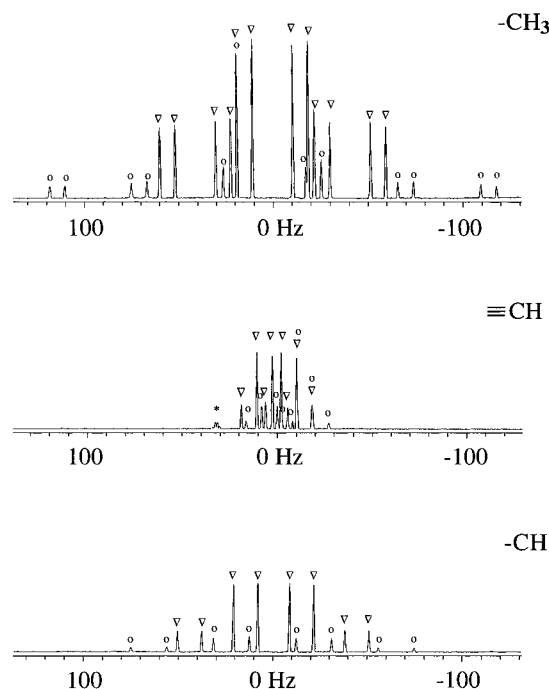


Figure 2. 400 MHz 1H NMR subspectra of the methyl group, H5 and H6 protons obtained by recording 32 FID signals with 16K of data points (SW = 2000 Hz). Zero filling to 32K data points was used to increase the digital resolution to 0.12 Hz/point. An unshifted sine-bell filtering and a base line correction were also applied to enhance the spectral appearance. An average line width of 1.5 Hz at half maximum was measured. (∇) *S* enantiomer; (\circ) *R* enantiomer; (*) chemical impurity. For each proton subspectrum, the center is shown here as 0 Hz. The relative chemical shifts are given in Table 1.

tickling experiments.¹⁰ The iterative analyses gave a maximum deviation in line position between the simulated and experimental spectra of smaller than 0.12 Hz for both enantiomers, and the root mean square (rms) errors of the fits were equal to 0.05 and 0.03 Hz for the *R* and *S* isomers, respectively. The chemical shift of protons and the chemical shift differences between the *R* and *S* enantiomers are summarized in Table 1. We may note here the large difference of chemical shift of H5 in the two enantiomers, which is a consequence of the large chemical shift anisotropy of the acetylenic proton. Recently,

TABLE 1: Chemical Shifts of Protons and Carbons for Each Enantiomer of (±)-BTL

atoms ^a	ν_i^R (in ppm)	ν_i^S (in ppm)	$ \nu_i^R - \nu_i^S $ (in Hz)
C ₁ ^c	24.22	24.19	3.0
C ₂	57.87	57.88	1.0
C ₃	nd ^b	85.28	nd
C ₄	71.38	71.58	20.1
H ₅ ^d	1.66	1.65	5.0
H ₆	3.75	3.75	0.2
H _(6,7,8)	0.68	0.68	0.2

^a See Figure 1 for the atom numbering. ^b No experimental data. ^c The C-13 signal of chloroform was used as internal reference and assigned to 77.0 ppm. ^d The H-1 signal of chloroform was used as internal reference and assigned to 7.24 ppm.

the $\Delta\sigma_H$ of acetylene was measured, and a value of 17.1 ppm was obtained.¹¹ The data from the proton analysis are listed in Table 2.

Carbon-13 Spectral Analysis. The ¹³C spectrum is presented in Figure 3. It was analyzed by keeping the ¹H–¹³C scalar couplings equal to their isotropic values, and maintaining unchanged the ¹H–¹H scalar and dipolar couplings during the fitting processes. The signs of the ¹J_{CH} can be safely assumed to be positive, which then allowed the magnitude and sign of the ¹D_{CH} to be determined.¹² The determination of the magnitude and sign of long range dipolar couplings, i.e. ^{2,3,4}D_{CH}, was more of a problem since the signs of the scalar couplings ^{2,3,4}J_{CH} are not certain. To overcome this problem, a set of seven *D_{ij}* (four *D_{HH}* and three *D_{CH}*), which are determined reliably from the spectra, because the signs of the corresponding *J_{ij}* are known, were used to calculate an approximate set of order parameters. Having obtained the elements *S_{αβ}^R* and *S_{αβ}^S*, they are then used to calculate the ^{2,3,4}D_{CH} whose signs and magnitudes were previously in doubt. Having a good approximation to the magnitudes of the ^{2,3,4}D_{CH} enabled the signs of the corresponding *J_{ij}* to be determined. Knowing now the signs and magnitudes of the *J_{ij}*, and the signs of the ^{2,3,4}D_{CH} allowed the magnitudes of these dipolar couplings to be obtained from the spectral analyses. The agreement obtained between observed and calculated line positions in the carbon spectrum was 0.25 Hz and 0.20 Hz for the *R* and *S* enantiomers, respectively. The chemical shift of carbons and the dipolar couplings obtained from the carbon-13 spectra are reported in Tables 1 and 2. Note that signals from C3 for the *R* isomer were not observed in the spectrum since these are obscured by the more intense peaks from the *S* enantiomer. Consequently, while 12 ¹³C–¹H dipolar couplings were extracted from the carbon-13 spectrum analysis for the *S* isomer, only 9 were obtained for *R*.

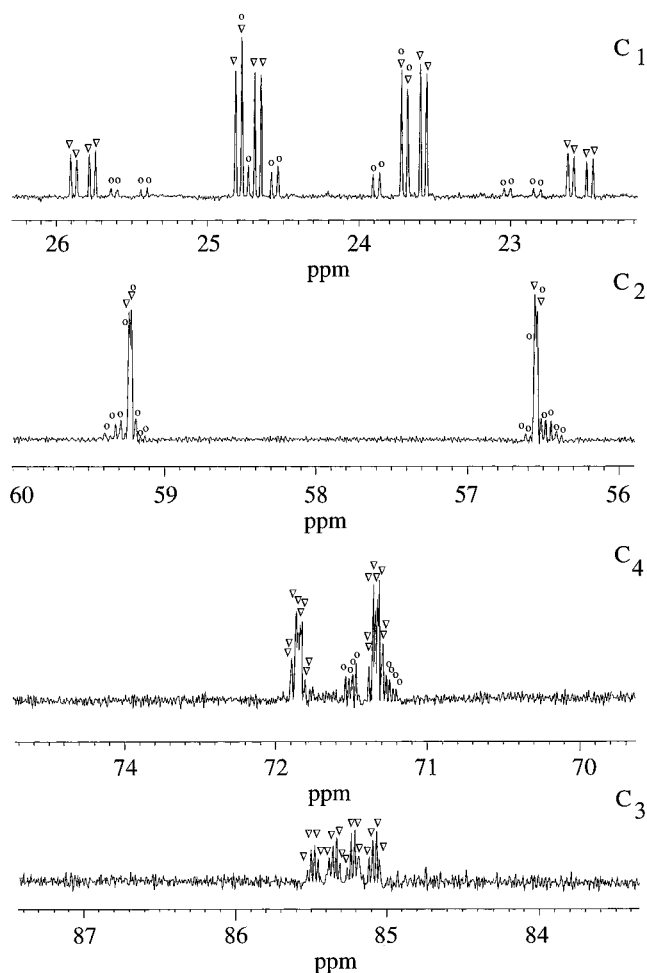


Figure 3. 100 MHz ¹³C NMR subspectra of the C1, C2, C4, C3 carbons obtained by recording 1500 FID signals with 16K of data points (SW = 7812.5 Hz). Zero filling to 32K data points was used to increase the digital resolution to 0.48 Hz/point. An unshifted sine-bell filtering and a base line correction were also applied to enhance the spectral appearance. An average line width smaller than 2 Hz at half-maximum was measured. The carbon-13 signal of the CDCl₃ was used as internal reference and assigned the value of 77.0 ppm. (∇) *S* enantiomer, (○) *R* enantiomer. Note that the signals of the C3 carbon for the *R* enantiomer were not observed on the spectrum.

In conclusion, a set of 13 and 16 dipolar couplings for the *R* and *S* enantiomer was obtained and used in the subsequent analyses to determine the structure and orientational order of the two isomers.

TABLE 2: Experimental Scalar and Dipolar Couplings Measured on the ¹H and ¹³C Spectra (in Hz)

type of atoms	numbering of atoms ^a	number of bonds	$J_{ij}^{iso\ b}$	$(D_{ij}^{exp})\ R\ ^b$	$(D_{ij}^{exp})\ S\ ^b$
C··H	1–5	4	-1.45 ± 0.04	-1.37 ± 0.02	-1.37 ± 0.02
C··H	1–6	2	-3.92 ± 0.02	11.68 ± 0.04	8.22 ± 0.03
C··H	1–(7,8,9)	1	128.57 ± 0.03	-20.92 ± 0.03	-9.33 ± 0.03
C··H	2–5	3	3.42 ± 0.02	-3.44 ± 0.02	-2.67 ± 0.02
C··H	2–6	1	147.96 ± 0.03	65.12 ± 0.03	60.49 ± 0.03
C··H	2–(7,8,9)	2	-4.69 ± 0.03	5.82 ± 0.02	2.34 ± 0.02
C··H	3–5	2	48.44 ± 0.03	nd ^c	-10.87 ± 0.02
C··H	3–6	2	-6.09 ± 0.03	nd ^c	-4.11 ± 0.02
C··H	3–(7,8,9)	3	5.41 ± 0.02	nd ^c	-1.52 ± 0.03
C··H	4–5	1	249.86 ± 0.02	-136.26 ± 0.04	-99.18 ± 0.04
C··H	4–6	3	3.60 ± 0.04	-4.06 ± 0.03	-2.39 ± 0.03
C··H	4–(7,8,9)	4	0.0 ± 0.20	-1.11 ± 0.03	-1.44 ± 0.03
H··H	5–6	4	-2.10 ± 0.03	-8.23 ± 0.04	-5.35 ± 0.02
H··H	5–(7,8,9)	5	0.00 ± 0.02	-4.05 ± 0.02	-4.07 ± 0.02
H··H	6–(7,8,9)	3	6.57 ± 0.03	18.64 ± 0.02	11.46 ± 0.02
H··H	(7,8,9)	2	nd ^c	-30.71 ± 0.02	-13.65 ± 0.02

^a See Figure 1 for the atom numbering. ^b Experimental fitted values from the program PANIC. ^c No experimental data.

TABLE 3: Structural Parameters of (\pm)-BTL Derived from Geometrical Data Reported in Ref 13

parameters	value
R_{13}/R_{12}^a	1.604
R_{14}/R_{12}	2.289
R_{15}/R_{12}	2.966
R_{16}/R_{12}	1.408
R_{17}/R_{12}^b	0.712
angle C1–C2–C3	110.50° ^c
angle C1–C2–H6	109.47°
angle C2–C3–C4	180°
angle C2–C1–H(7,8,9)	109.47°
angle C3–C4–H5	180°

^a $R_{12} = 1.535$ Å. ^b $R_{17} = R_{18} = R_{19}$. ^c Angle determined by microwave spectroscopy.

TABLE 4: Elements, $S_{\alpha\beta}^k$, of the Order Tensor for the *R* and *S* Enantiomers Calculated from the Experimental Set and Vibrationally Corrected Set of Dipolar Couplings

parameters	no vibrational corrections		vibrational corrections	
	<i>R</i> enant.	<i>S</i> enant.	<i>R</i> enant.	<i>S</i> enant.
S_{aa}^a	−0.002 84	−0.001 26	−0.002 86	−0.001 26
S_{ab}	−0.000 65	0.000 43	−0.000 56	0.000 23
S_{ac}	−0.002 38	−0.002 67	−0.002 50	−0.002 99
S_{bc}	−0.001 53	0.001 38	−0.001 37	0.001 39
S_{cc}	0.004 75	0.002 65	0.005 40	0.002 78
rms ^b	0.448	0.295	0.158	0.143

^a The $S_{\alpha\beta}$ values are reported with respect to the reference molecular axis system shown in Figure 1. ^b Root mean square deviation in Hz.

Discussions

Our aim is to establish whether the enantiomers when bound to the PBLG have identical geometries and to characterize their order matrices. We also wish to establish the effect on the derivation of the order matrices of adopting a model geometry that is identical for each enantiomer. We shall then proceed to show the importance of correcting the dipolar couplings for vibrational motion.

The Model Molecular Geometry. The bond lengths and angles are given in Table 3 and are those used by Marstokk and Møllendal to analyze the microwave spectrum of (\pm)-BTL.¹³ Note that the C2–C3–C4–H5 fragment is assumed to be linear. The only geometrical parameter that was optimized to fit the microwave data is the C1–C2–C3 angle.

The methyl group is assumed to have a 3-fold symmetry axis coincident with C1–C2. The barrier to rotation of methyl groups with a 3-fold, rather than a 6-fold symmetry axis is generally of the order of 12 kJ·mol^{−1}, and so at 300 K the protons in this group can be assumed to spend all their time in the three equivalent minimum energy positions generated by rotation through 120°. The motion of the methyl group is therefore equivalent to jumps between these three sites.¹⁴ In this model geometry the location of the methyl protons is such that the C1–H7 bond in Figure 1 lies in the *ac* plane.

Two reference molecular axis systems (*a*, *b*, *c*)^R and (*a*, *b*, *c*)^S associated with the *R* and *S* isomers were defined as displayed in Figure 1. Note that the *R* and *S* enantiomers are mirror images of one another relative to the *ac* plane.

Calculation of the Order Parameters with the Model Geometry. With the model geometry for both isomers, the five independent order parameters $S_{\alpha\beta}^k$ were obtained from eq 2 by a least-squares fitting method using the program SHAPE developed by Diehl *et al.* and internally modified to take into account the averaging produced by the rotation of the methyl group.¹⁵ The values obtained for the $S_{\alpha\beta}^k$ are shown in Table 4. The errors on the $S_{\alpha\beta}^k$ were estimated to be smaller than 5×10^{-5} .

Some of the differences, ΔD_{ij}^k , between the calculated and experimental D_{ij} are unacceptably large, and possible ways of reducing their magnitudes were explored. Thus, the assumption that the C1–H7 bond lies in the *ac* plane was relaxed, and a rotation through a fixed angle ϕ^k about the C1–C2 bond included as a variable in the minimisation procedure, while retaining the 3-fold symmetry of the group. This did not, however, lead to a significant change in the ΔD_{ij}^k , and the data supports a value of $\phi^k = 0^\circ$ for the two enantiomers.

The possibility was also explored that the methyl rotates freely about the C1–C2 bond. In principle this would lead to order parameters which are dependent on ϕ^k , and the calculation of these would require adopting a model for this phenomenon.^{16,17} However, the dependence of order parameters on methyl group rotation is expected to be small, and was neglected. These calculations involved averaging the couplings to the methyl protons over all values of ϕ^k being equally probable. It did not lead to a change in the quality of the agreement between observed and calculated dipolar couplings. Consequently, the large values of the ΔD_{ij}^k could arise because the model geometry is incorrect, but including the positions of the interacting nuclei in the minimization procedure leads to a grossly distorted structure. It was concluded, therefore, that the disagreement between the observed and calculated dipolar couplings arises because of the neglect of vibrational averaging.

Calculation of the Structure r_α and Orientational Order from Vibrationally Corrected Dipolar Couplings. Vibrational averaging is known to have an appreciable effect on dipolar couplings, and in particular on $^1D_{CH}$. To calculate these effects is not a trivial task. Even if the calculations neglect the contribution from anharmonicity, there remains the problem of how the orientational order is coupled to the vibrational motion. This is the effect that produces a dipolar splitting, for example, between the protons in methane dissolved in a liquid crystalline solvent, even though the equilibrium structure of this molecule precludes the possibility of orientational ordering. It is difficult to calculate these deformation effects *a priori*, and since they are usually small, they are neglected here. With these simplifying assumptions the corrected dipolar couplings, $(D_{ij}^k)^{corr}$, are then given by¹⁸

$$(D_{ij}^k)^{corr} = (D_{ij}^k)^{exp} - (D_{ij}^k)^{harm} \quad (3)$$

To calculate $(D_{ij}^k)^{harm}$, it is necessary to know the vibrational wavefunctions, φ_v , for the chiral compound, which will be the same for the two isomers. The normal route to obtaining the φ_v is to derive a force field by fitting observed and calculated vibrational frequencies.^{18,19} Harmonic corrections to the dipole–dipole couplings were computed with the program VIBR. As no experimental force field for (\pm)-BTL could be found in the literature, the force constants were calculated by applying a semiempirical molecular orbital method based on three different levels of approximation, referred as AM1, PM3, and MN-DOC.^{20–22} The program VIBR was written initially to use a force field given in an internal valence coordinate system. In the present calculation, the force constant matrix was directly produced in cartesian coordinates, and therefore, 'VIBR' had to be modified. The current modified version has two significant advantages: first the confusion often present when internal coordinates (or symmetrized internal coordinates) are applied can now be avoided; second, as “good” force fields can be obtained by *ab initio* or semiempirical calculations, they can be fed directly into VIBR, and the vibrational corrections are obtained immediately. The performance of the modified VIBR program and the “quality” of the force field derived at different approximations were checked by using benzene as a test case.

TABLE 5: Final Values of the Fitting Parameters Obtained after Three Refinements of the Vibrational Corrections

parameters	initial	<i>R</i> enantiomer		<i>S</i> enantiomer	
	geom.	final geom.	[%] ^c	final geom.	[%] ^c
$\angle\text{C2-C1-H}(7,8,9)^a$	109.47	111.4	1.8	111.6	1.9
$d_{(4-5)}^b$	1.060	1.118	5.1	1.110	4.5

^a Angle (in deg). ^b Distance (in Å). ^c Relative error in percent (Δ value/corrected value).

TABLE 6: Dipolar Couplings Corrected for Harmonic Vibrations and Difference between Corrected and Calculated Values using SHAPE (in Hz)

atom ^a	$(D_{ij}^R)^{\text{corr } b}$	$\Delta D_{ij}^{R, c}$	$(D_{ij}^S)^{\text{corr}}$	ΔD_{ij}^S
1-5	-1.36	0.11	-1.37	-0.03
1-6	11.73	-0.42	8.22	-0.10
1-(7,8,9)	-19.82	0.03	-8.65	0.00
2-5	-3.42	-0.06	-2.66	-0.24
2-6	68.45	0.01	62.58	-0.02
2-(7,8,9)	5.82	0.22	2.32	-0.14
3-5	nd ^d	nd	-10.68	-0.22
3-6	nd	nd	-4.23	0.23
3-(7,8,9)	nd	nd	-1.51	0.20
4-5	-130.33	0.00	-94.98	0.02
4-6	-4.08	0.27	-2.41	0.07
4-(7,8,9)	-1.10	0.20	-1.43	0.14
5-6	-8.23	-0.17	-5.36	-0.38
5-(7,8,9)	-4.07	-0.11	-4.04	-0.12
6-(7,8,9)	18.54	0.09	11.40	0.04
(7,8,9)	-31.37	-0.03	-13.91	0.00

^a See Figure 1 for the atom numbering. ^b Dipolar couplings corrected for vibrational motions. ^c Difference between the calculated and corrected values: $\Delta D_{ij}^k = (D_{ij}^k)^{\text{corr}} - (D_{ij}^k)^{\text{calc}}$. ^d No experimental data.

For (\pm)-BTL the final corrections were practically independent of the level of approximation used in the molecular orbital calculations, and consequently only the results at the PM3 level are considered here. In the computation, the conformation depicted in Figure 1 was adopted. Finally, it should be noticed that the lowest vibrational modes (below 200 cm^{-1}) were omitted, because they are related to the large amplitude torsional motion of the methyl group, which cannot be treated on VIBR. The methyl group rotation was considered as in the text.

The five order parameters, the C4-H5 distance and the C2-C1-H(7,8,9) angle were used as fitting parameters, and three refinements of the vibrational corrections were made, using successively the VIBR and SHAPE programs. The results are shown in Tables 4, 5, and 6, respectively. As expected, the largest vibrational corrections were obtained on D_{45} and D_{26} couplings for both enantiomers. Note that the corrections to these two couplings are of opposite sign. This is because the vibrational corrections depend on the orientational order parameters as well as on the vibrational amplitudes. The new geometrical data are in a fully acceptable range and are essentially identical for the two enantiomers. The calculated and vibrationally corrected dipolar couplings are now in a very close agreement, as shown in Table 6. The biggest relative difference ($\approx 14\%$) is obtained for $D_{4-(7,8,9)}$. It is possible that this discrepancy arises because $^4J_{4-(7,8,9)}$ could not be accurately determined from the isotropic carbon-13 spectrum. In fact, the isotropic spectrum of the C4 carbon appears to be a large doublet of doublets and not a doublet of doubled quartets as expected, the difference being caused by the overlapping of lines. The error on $^4J_{4-(7,8,9)}$ was estimated to be ± 0.2 Hz, corresponding approximately to the difference between the calculated and corrected dipolar couplings given in Table 6.

Determination of the Principal Order Matrices and Eigenvectors. Our aim is now to quantify the differential ordering effect (DOE) between the two enantiomers. For this purpose, the order matrices in the $(a,b,c)^k$ reference frame were

TABLE 7: Principal Components, $S_{\alpha\alpha'}$, of the Diagonalized Matrix and Biaxiality Term for the *R* and *S* Enantiomers

parameters ^a	<i>R</i> enantiomer	<i>S</i> enantiomer
$S_{a'a'}$	-0.004 13	-0.003 30
$S_{b'b'}$	-0.002 13	-0.001 34
$S_{c'c'}$	0.006 26	0.004 64
$S_{b'b'} - S_{a'a'}$	0.002 00	0.001 96

^a The $S_{\alpha\alpha'}$ value are reported with the respect to the principal axis system described in Figure 4.

TABLE 8: Quantification of the DOE in Terms of Angular Differences and Euler Angles (in deg)

type	parameter	no vibrational corrections	vibrational corrections
angular diff. ^a	θ_{RS}'	11 ± 1	11 ± 1
	θ_{RS}''	7 ± 0.7	4 ± 0.4
	θ_{RS}'''	10 ± 1	12 ± 1
Euler	θ_{RS}	10 ± 1	12 ± 1
	ϕ_{RS}	-22 ± 2	-18 ± 2
	χ_{RS}	27 ± 3	17 ± 2

^a Angular difference between the a' , b' , and c' axes of the (*R*)-PAS and (*S*)-PAS.

diagonalized using the program MATHEMATICA to give both their values $S_{\alpha\alpha'}$ in the principal frame, $(a',b',c')^k$, and the eigenvectors (a',b',c') associated with each enantiomer.⁶ The three nonzero diagonalized order parameters are shown in Table 7 together with the biaxiality term, $S_{b'b'} - S_{a'a'}$, in the ordering.²³ The relative difference of orientation between the (*R*)-PAS and (*S*)-PAS could be then expressed in terms of angular differences between each axis of the two frames and in terms of Euler angles θ , ϕ , χ .²⁴ These are given in Table 8. Note that only the directions of the eigenvectors can be directly defined by the calculations; consequently the final eigenvector orientation for the two PAS was chosen in order to have an opposite handedness and an opposite orientation relative to the ac plane. The orientational principal axes $(a',b',c')^S$ and $(a',b',c')^R$ are displayed relative to the reference frame in Figure 4. Consequently, before both molecular frames were compared, the (*R*)-PAS was inverted with respect to the ac plane in order for it to have the same handedness as the (*S*)-PAS.

Tables 7 and 8 reveal some noticeable results. First, the molecular orientational order is not biaxial, i.e. $S_{a'a'} \neq S_{b'b'} \neq -S_{c'c'}/2$.²⁵ Second, the ratios $(S_{b'b'} - S_{a'a'})/S_{c'c'}$ are different for the two enantiomers (0.319 for *R* and 0.423 for *S*). This shows that the principal order parameters for the *R* and *S* enantiomers are not linearly related. Third, the nonzero values for the angular differences and Euler angles demonstrate clearly that the PAS of the *R* and *S* enantiomers are not mirror images relative to the ac plane. Consequently, the difference in absolute value of the order parameters could not arise only from differences in the fraction, p^k , of bound molecules. These results are a clear indication that the *R* and *S* isomers do not have the same orientation when bound to the solvent molecules. Such a conclusion reveals that the molecular shape of chiral solutes plays an important role in the chiral recognition mechanisms in PBLG. This conclusion confirms the results first obtained in the case of the (\pm)-TMPL and shows that the chiral recognition mechanisms involved with PBLG are very similar for these two investigated examples.

Finally, the analysis of data from Table 8 shows that the orientation of the two frames are very comparable when the experimental and vibrationally corrected dipolar couplings are used. The larger apparent differences obtained for the ϕ and χ angle are due to the high "sensitivity" of these angles to a small angular variation of PAS.

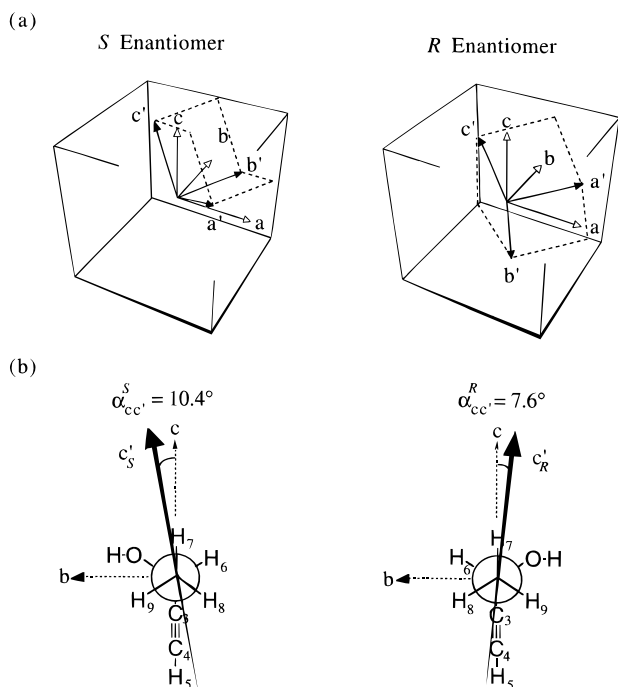


Figure 4. (a) Space representation of the (*R*)-PAS and (*S*)-PAS of (\pm)-BTL. The eigenvectors associated to the eigenvalues of the diagonal matrices are orthonormal. (b) Representation of the major orientation axis (c') relative to the ac plane. The angle α between the ac plane and the c' axis is 7.6° and 10.4° for the *R* and *S* enantiomers, respectively.

Conclusion

The dipolar couplings for the *R* and *S* isomers of (\pm)-BTL are consistent with there being no change in their structure on binding to PBLG. This conclusion could be reached only by including the effects of vibrational averaging, even if at an approximate level, into the analysis of the data. The inclusion of vibrational averaging also allows more precise values for the order parameters to be obtained, although now the effect, although large, is not so dramatic. Indeed, if the two isomers are assumed to have the same structure, even an approximate one such as the starting model geometry used for (\pm)-BTL, this gives the same qualitative result for the order matrices as when the vibrational corrections are done, and the geometry is optimized. Thus, the relative magnitude of the principal order parameters is the same, as too are the relative orientations of the principal axes.

This new investigation demonstrates that the *R* and *S* isomers of the (\pm)-BTL are clearly oriented on average differentially in the PBLG medium, thus giving support to conclusions reached first in the case of (\pm)-TMPL. Such a conclusion reveals therefore that the molecular shape recognition phenomenon plays an important role in the general process of chiral recognition. The PBLG system can be regarded as being like any natural biopolymer system, which gives rise to a helical structure such as DNA. Consequently, the classical models involved for enzyme enantioselectivity might furnish a good starting point to understand the enantiomeric discrimination phenomenon involved with PBLG.²⁶

One should note, however, that the results reported here may be specific to (\pm)-BTL. It is indeed surprising that the dipolar couplings for the nuclei in such a small molecule interacting with a large polymer such as PBLG are apparently free from

some of the effects that have been observed for other solute–liquid crystalline solvent systems. Thus, to quote an extreme example, the dipolar couplings between the nuclei in acetylene dissolved in the liquid crystalline solvent are not consistent with a linear geometry.²⁷ This has been interpreted as showing that the acetylene interacts with at least two sites on the liquid crystalline solvent molecules, and the order parameters at the two sites have opposite signs.

Rather smaller effects have been noted for other molecules, in that the geometries obtained by analyzing sets of dipolar couplings obtained on solutions in several different liquid crystalline solvents are not consistent with a single structure. This is caused by the orientation–vibration correlation, or deformation effect noted earlier. It is possible that such effects are operating with PBLG as a solvent, and their detection and characterization presents a formidable challenge.

Acknowledgment. The authors thank Dr. Y. Gounelle and Prof. A. Loewenstein for their many helpful and enlightening discussions and Dr. W. Smadja who has kindly provided the sample of (\pm)-3-butyn-2-ol. P.L. acknowledges the Royal Society of London for funding a postdoctoral fellowship during one year at the University of Southampton, and the French Foreign Office for the award of a “Lavoisier” grant.

References and Notes

- (1) Meddour, A.; Canet, I.; Loewenstein, A.; Péchiné, J. M.; Courtieu, J. *J. Am. Chem. Soc.* **1995**, *116*, 9652.
- (2) Lesot, P.; Meddour, A.; Loewenstein, A.; Courtieu, J. *J. Chem. Soc., Faraday Trans.* **1995**, *91* (9), 1371.
- (3) Canet, I.; Courtieu, J.; Loewenstein, A.; Meddour, A.; Péchiné, J. M. *J. Am. Chem. Soc.* **1995**, *117*, 6520.
- (4) Meddour, A.; Berdagué, P.; Hedli, A.; Courtieu, J.; Lesot, P. *J. Am. Chem. Soc.* **1997**, *119*, 4502.
- (5) Emsley, J. W.; Lindon, J. C. In *NMR Spectroscopy Using Liquid Crystal Solvents*; Pergamon Press: Oxford, 1975.
- (6) Lesot, P.; Gounelle, Y.; Merlet, D.; Loewenstein, A.; Courtieu, J. *J. Phys. Chem.* **1995**, *99*, 14871; (additive corrections) **1995**, *100*, 14569.
- (7) Michelet, V.; Besnier, I.; Tanier, S.; Touzin, A. M.; Genet, J. P., Demoute, J. P. *Synthesis* **1995**, 165.
- (8) Lesot, P.; Merlet, D.; Courtieu, J.; Emsley, J. W. *Liq. Cryst.* **1996**, *21* (3), 427.
- (9) Emsley, J. W.; Feeney, J.; Sutcliffe, L. H. In *High resolution NMR Spectroscopy*; Pergamon Press: Oxford, 1965; Vol. 1.
- (10) Freeman, R. *Mol. Phys.* **1961**, *4*, 385.
- (11) Kaski, J.; Lantto, P.; Vaara, J.; Jokisaari, J. **1997**, to be submitted.
- (12) Kalinowski, H. O.; Berger, S.; Braun, S. In *Carbon-13 NMR Spectroscopy*; Wiley and Sons: Chichester, 1984.
- (13) Marstokk, K. M.; Møllendal, H. *Acta Chem. Scand.* **1985**, *A39*, 639.
- (14) Emsley, J. W. In *Encyclopedia of NMR*; Grant, D. M., Harris, R. K., Eds.; John Wiley & Sons: Chichester, 1996; p 2781.
- (15) Diehl, P.; Henrichs, P. M.; Niederberger, W. *Mol. Phys.* **1971**, *20* (1), 139.
- (16) Lin, C. C.; Swallen, J. D. *Rev. Mod. Phys.* **1959**, *31*, 841.
- (17) Lowe, J. L. *Phys. Org. Chem.* **1968**, *6*, 1.
- (18) Sykora, S.; Vogt, J.; Bosiger, H.; Diehl, P. *J. Mag. Res.* **1979**, *36*, 53.
- (19) Wasser, R.; Diehl, P. *J. Magn. Reson.* **1989**, *81*, 121 and references cited therein.
- (20) Dewar, M. J. S. *J. Mol. Struct.* **1988**, *180*, 1.
- (21) Thiel, W. *J. Am. Chem. Soc.* **1981**, *103*, 1413.
- (22) Steward, J. *J. Comput. Chem.* **1989**, *10*, 209; **1991**, *12*, 320.
- (23) Sander, C. R., II; Hare, B. J.; Hord, K. P.; Prestegard, J. H. *Prog. NMR Spectrosc.* **1994**, *26* (5), 421.
- (24) Zare, R. N. In *Angular momentum, Understanding Spatial Aspects in Chemistry and Physics*; John Wiley & Sons: New York, 1988.
- (25) Dayan, S.; Fried, F.; Gilli, G. M.; Sixou, P. *J. Polym. Sci. Symp.* **1983**, *37*, 193.
- (26) Fitzpatrick, A.; Klivanov, A. M. *J. Am. Chem. Soc.* **1991**, *113*, 3166.
- (27) Diehl, P.; Sykora, S.; Niederberger, W.; Burnell, E. E. *J. Magn. Reson.* **1974**, *14*, 260.